BNL-98468-2012-CP

Structural- and optical-properties of CdTe and CdMnTe films

Aleksey E. Bolotnikov

Presented at the 2012-SPIE Optics & Photonics Conference
San Diego, CA
August 12-16, 2012

August 2012

Nonproliferation and National Security Department

Brookhaven National Laboratory

P.O. Box 5000
Upton, N.Y. 11973-5000
www.bnl.gov

DISCLAIMER

Structural- and optical-properties of CdTe and $Cd_xMn_{1-x}Te$ films

A. S. Opanasyuk[a], P. V. Koval[a], V. V. Kosyak,[b], P. M. Fochuk[c], A. E. Bolotnikov[d], and R. B. James[d]
[a]Sumy State University, Ukraine; [b]Department of Materials Science & Engineering, University of Utah, USA; [c]Chernivtsy National University, Ukraine; [d]Brookhaven National Laboratory, USA

ABSTRACT

We undertook a detailed investigation of the structural- and optical-properties of CdTe- and $Cd_{1-x}Mn_xTe$-semiconductor films deposited by close-spaced vacuum sublimation using thermal evaporation on non-oriented substrates. From our structural- and phase-analysis of the layers, we obtained information on their structure, deformations, grain size, and content of dislocations for films deposited at different substrate temperatures. We considered that despite the presence of defects in the crystals, the films offer promise for fabrication into x-ray detectors.

Keywords: CdTe, $Cd_{1-x}Mn_xTe$, structural analyses, scattering domains, micro-deformations, transmission- and reflection-spectra, wide band-gap semiconductors

INTRODUCTION

High-resistivity CdTe single crystals are used widely as detectors for hard X-ray radiation [1-2]. Recently, CdTe-based solid solutions ($Cd_{1-x}Zn_xTe$ and $Cd_{1-x}Mn_xTe$) were deemed as more promising materials for such detectors than chlorine-doped CdTe crystals. Moreover, $Cd_{1-x}Mn_xTe$ solid solution has several significant advantages over $Cd_{1-x}Zn_xTe$, namely a low segregation coefficient ($k \approx 1$) for Mn, and high sensitivity of the band-gap (BG) value to the doping rate. For example, it is about 13 meV per 1 at.% of Mn, whereas for $Cd_{1-x}Zn_xTe$ it is only 6.7 meV per 1 at.% of Zn. Furthermore, doping the CdTe with about 6% of Mn, such that the concentration of the dopant is two times lower than for Zn in CZT, yields solid solutions with a band-gap width, E_g, up to 1.60 eV and a resistivity of 10^{10}-10^{11} Om·cm. Also, the value of the product of the mobility and free-carrier lifetime, $\mu\tau$, remains reasonably high. In addition, there is a lower probability of twins and Te precipitates compared with other detector materials [3-4].

To reduce the cost of detectors, others have proposed using thick (up to 100 μm) epitaxial- or polycrystalline-films rather than expensive CdTe single crystals [5-6]. While $Cd_{1-x}Mn_xTe$ films also might be promising as a detector material, the properties of thick compound- and ternary-films have not been well studied.

In comparison with our information of the properties of $Cd_{1-x}Mn_xTe$ single crystals [7-10], there is a dearth of data on $Cd_{1-x}Mn_xTe$ films. This lack might be attributed to the complexity of depositing the films due to the significant difference in vapor pressure of the components. Therefore, in most cases, for obtaining $Cd_{1-x}Mn_xTe$ films, laser deposition, flash evaporation, and magnetron sputtering are used [11-13]; therein, highly non-equilibrium conditions are typical, so leading to films of low quality that are unsurprisingly inadequate for high-performance radiation-detection devices.

The aim of our work was to detail the influence of growth conditions on the chemical composition, structural- and optical-properties of CdTe and $Cd_{1-x}Mn_xTe$ films obtained by closed-space vacuum sublimation (CSVS) [14].

EXPERIMENTAL METHODS

Thin CdTe films and $Cd_{1-x}Mn_xTe$ films (d = 0.5-5 μm) were deposited on cleaned glass substrates by the CSVS method in a vacuum chamber under a residual gas pressure of about $6 \cdot 10^{-3}$ Pa. We note that thin films were used for our optical studies, and thick layered ones for our structural analyses. To deposit CdTe films, we used various substrate temperatures, T_s, ranging from 20- to 550- ^{0}C and an evaporator temperature, T_e, of 620 ^{0}C. The $Cd_{1-x}Mn_xTe$ was deposited by evaporating the $Cd_{0.7}Mn_{0.3}Te$ powder and co-evaporating the CdTe and Mn powders. To prevent re-evaporation, the substrate temperature at which we deposited the thin films from the $Cd_{0.7}Mn_{0.3}Te$ powder was 150 ^{0}C, while the evaporator temperature ranged from 650- to 850-^{0}C. For co-evaporating CdTe and Mn, the substrate

temperature was raised from 350- to 550-^{0}C, and the Mn- and CdTe- source temperatures, respectively, were 850 ^{0}C and 700 ^{0}C. We studied the films' surface morphology by scanning electron microscopy (SEM). The average grain size (D) was determined by the Jeffries method [15], while the thickness of the films was measured by the interference method and from the SEM images of their cross-section.

The structural analysis of the thin films was carried out with a DRON 4-07 X-ray diffractometer using a Ni-filtered $K_{\alpha Cu}$ radiation source in the range of diffraction angles 2θ from 20^0 to 80^0, where 2θ is the Bragg angle.

Phase analysis was undertaken via comparisons of the interplane distances and relative intensities of the films and the JCPDS reference data [16]. To determine the precise values of the lattice parameter, we used the Nelson-Riley extrapolation method [17-19].

We also employed the X-ray diffraction method in determining the size (L) of the coherent scattering domain (CSD) and the level of micro-deformations (ε) in CdTe films with respect to the broadening of the diffraction peaks. Cauchy- and Gauss-approximations were used to separate physical broadening of the diffraction lines, β, and tool broadening b. We applied the Hall approximation to separate the contributions to physical broadening caused by the dispersive CSD β_L and micro-deformation β_ε. To assure more accurate L and ε values, we used the three-fold convolution method. The mean dislocation density was calculated according to the micro-deformation level and CSD size following a method described by others [19-20]. We previously detailed our methods of analyzing the X-ray data [14, 21-22].

The samples' chemical compositions were studied by energy dispersive X-ray (EDAX) and proton-induced X-ray emission (PIXIE) methods, the experimental procedures for which were described in Refs. [21, 23-24].

The spectral dependencies of the reflection $R(\lambda)$ and transmission $T(\lambda)$ coefficients were measured by the SF-26 spectrophotometer in the wavelength λ range from 700- to 1000-nm. The adsorption coefficient of $Cd_{1-x}Mn_xTe$ and CdTe were calculated according to following equation $\alpha=-\frac{1}{d}\ln\left(\frac{1}{R^2}\left(-\frac{(1-R)^2}{2T}+\sqrt{\frac{(1-R)^4}{4T^2}+R^2}\right)\right)$ [7, 25].

RESULTS AND DISCUSSION

Figs. 1a and b, respectively, show the surface SEM image of a $Cd_{1-x}Mn_xTe$- and a CdTe-film. We determined that the growth mechanism of the films changes with increasing temperature. We observed the layer-by-layer growth of the fine-grained films obtained at a low substrate temperature T_s<1/3 T_m (where T_m is the melting point).

In contrast, films obtained at higher substrate temperatures have a column-like structure; the diameter of the columnar grains depends on the growth conditions and films' thickness (l) [14]. Furthermore, the size of the grains (D) increases with T_s and d; for example, thick CdTe films obtained at T_e = 620 ^{0}C and T_s = 550 ^{0}C have a $D \approx 70$ μm (Fig. 1b)

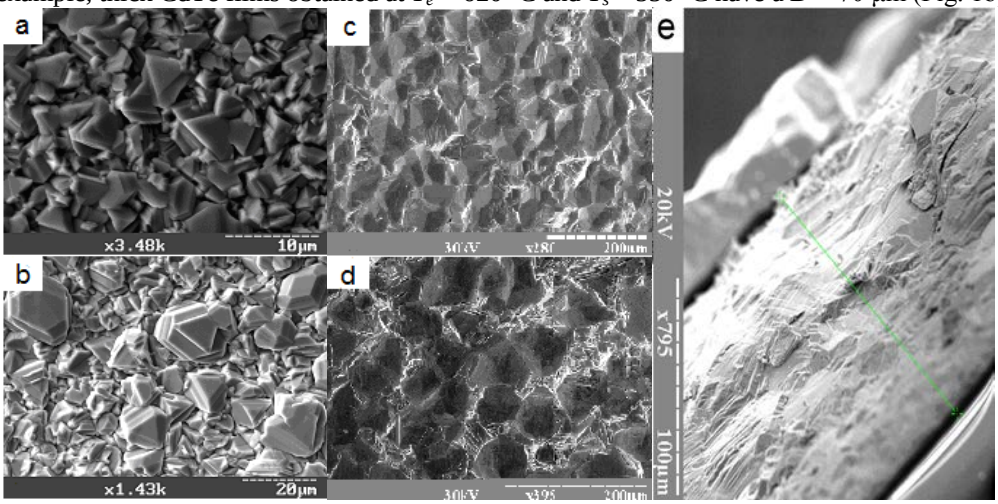

Figure 1. Surface SEM images of the films: (a) $Cd_{1-x}Mn_xTe$ film obtained at T_e = 800 ^{0}C and T_s = 525 ^{0}C, (b) $Cd_{1-x}Mn_xTe$ film obtained at T_e = 800 ^{0}C and T_s = 550 ^{0}C (c) CdTe obtained at T_e = 620 ^{0}C and T_s = 550 ^{0}C, (d) CdTe obtained at T_e = 620 ^{0}C and T_s = 500 ^{0}C and (e) cross-section of the CdTe film.

Traces of the hexagonal phase were detected in films obtained at T_s < 200-250 ^{0}C, whereas CdTe films deposited at higher substrate temperature (T_s = 300-550 ^{0}C) were cubic single phase.

Table 1 lists the values of the L and ε calculated for the CdTe films. The structural parameters calculated by the Gauss- and Cauchy-approximation are in good agreement. However, these methods allow us to determine only maximal values of the CSD sizes, L, and the minimal values of the micro-deformations, ε. More accurate calculations are provided by the three-fold convolution method [20-22], the results of which also are given in Table 1. We note that we carried out further calculations of the dislocation density according to the L and ε values assessed by the fold-convolution method.

Table 1. Sub-structural parameters of the CdTe films calculated according to different approximations for (111)-(222) planes.

T_s, ^{0}C	L, nm			$\varepsilon \cdot 10^3$			$\rho_{L\varepsilon}$, 10^{-14}, lin/m^2
	Approximation by		From convolution	Approximation by		From convolution	
	Gauss	Cauchy		Gauss	Cauchy		
CdTe							
150	60.6	64.5	61.0	1.11	1.22	1.07	7.0
250	64.5	74.5	64.9	0.94	0.74	0.64	4.0
350	85.7	99.1	86.7	0.88	0.23	0.65	3.0
425	74.8	86.6	75.3	0.87	0.30	0.71	3.8
450	72.3	81.5	72.9	0.93	0.22	0.68	3.7
550	56.6	51.2	56.9	1.02	0.75	0.69	4.9

Our analysis of the results for CdTe films shows that the SDS size along the direction normal to the (111) plane is maximal $L_{(111)}$~87 nm at 350 ^{0}C. The micro-deformation level monotonically decreases with substrate temperature from $1.10 \cdot 10^{-3}$ to $0.68 \cdot 10^{-3}$. A low incidence of dislocations $\rho_{L\varepsilon}$ = $3.0\text{-}7.0 \cdot 10^{-14}$ lin/m^2 is typical for all samples, wherein the minimal value ($\rho_{L\varepsilon}$=$3.0 \cdot 10^{-14}$ lin/m^2) corresponds to the 350 ^{0}C substrate temperature.

The chemical composition of the CdTe thin films was close to stoichiometric with C_{Cd}/C_{Te} = 0.98-1.01 (Table 2); moreover, the deviation from stoichiometry declines monotonically with rising substrate temperature for temperatures over 500 ^{0}C.

Table 2. Chemical composition of the CdTe and $Cd_{1-x}Mn_xTe$ films

T_s, ^{0}C	T_e, ^{0}C	T_{eMn} ^{0}C	wt. % Cd	wt. % Mn	wt. % Te	at. % Cd	at. % Mn	at. % Te	C_{Cd}/C_{Te}	C_{Cd+Mn}/C_{Te}	Notes
CdTe (EDAX)											
425	620	-	46.4	0	53.6	49.6	0	50.4	0.98		
450	620	-	47.4	0	53.6	49.6	0	50.4	0.98		
475	620	-	46.4	0	53.6	49.6	0	50.4	0.98		
500	620	-	46.4	0	53.6	49.6	0	50.4	0.98		
525	620	-	47.0	0	53.0	50.2	0	49.8	1.01		
550	620	-	46.9	0	53.2	50.0	0	50.0	1.00		
$Cd_{1-x}Mn_xTe$ (PIXE)											
450	800	-	45.0	0	55.0	48.2	0	51.8	0.93		Powder of $Cd_{1-x}Mn_xTe$
450	850	-	46.0	0	54.0	49.2	0	50.8	0.97		
350	620	850	28.0	11.7	60.4	26.6	22.8	50.6	0.53	0.98	Reg. 1
350	620	850	27.0	11.6	61.4	25.8	22.6	51.6	0.50	0.94	Reg. 2
450	620	900	45.3	0.5	54.2	48.2	1.0	50.8	0.95	0.97	
500	620	900	34.7	6.9	58.4	34.6	14.1	51.3	0.68	0.95	
550	620	900	43.3	1.6	55.1	45.5	3.4	51.0	0.89	0.96	

Accordingly, we conclude that thick CdTe films obtained at $T_s \geq 350$ ^{0}C are suitable for developing X-ray detectors, since the grain size therein is much more than the free carrier's drift length; also, these films have single-phase crystal structure and low concentration of dislocations.

The X-ray analysis of the $Cd_{1-x}Mn_xTe$ crystals shows that the main structure peculiarities of the ternary films are similar to those of CdTe films. However, the lattice parameter of the $Cd_{1-x}Mn_xTe$ films was somewhat more than in CdTe films; also, the $Cd_{1-x}Mn_xTe$ films have a lesser grain size D = (3-5) μm than the CdTe layers.

As the accuracy of the EDAX and PIXE methods is about 3-5%, we determined the concentration of Mn according to the relation between band-gap (BG) energy and dopant concentration. To study changes in the BG energy with the conditions under which the films were grown, we analyzed the samples' optical properties.

Figure 2 shows the spectral dependencies of the reflection $R(\lambda)$- and transmission $T(\lambda)$-coefficients measured for the $Cd_{1-x}Mn_xTe$ and CdTe films; pure CdTe films were used as reference samples.

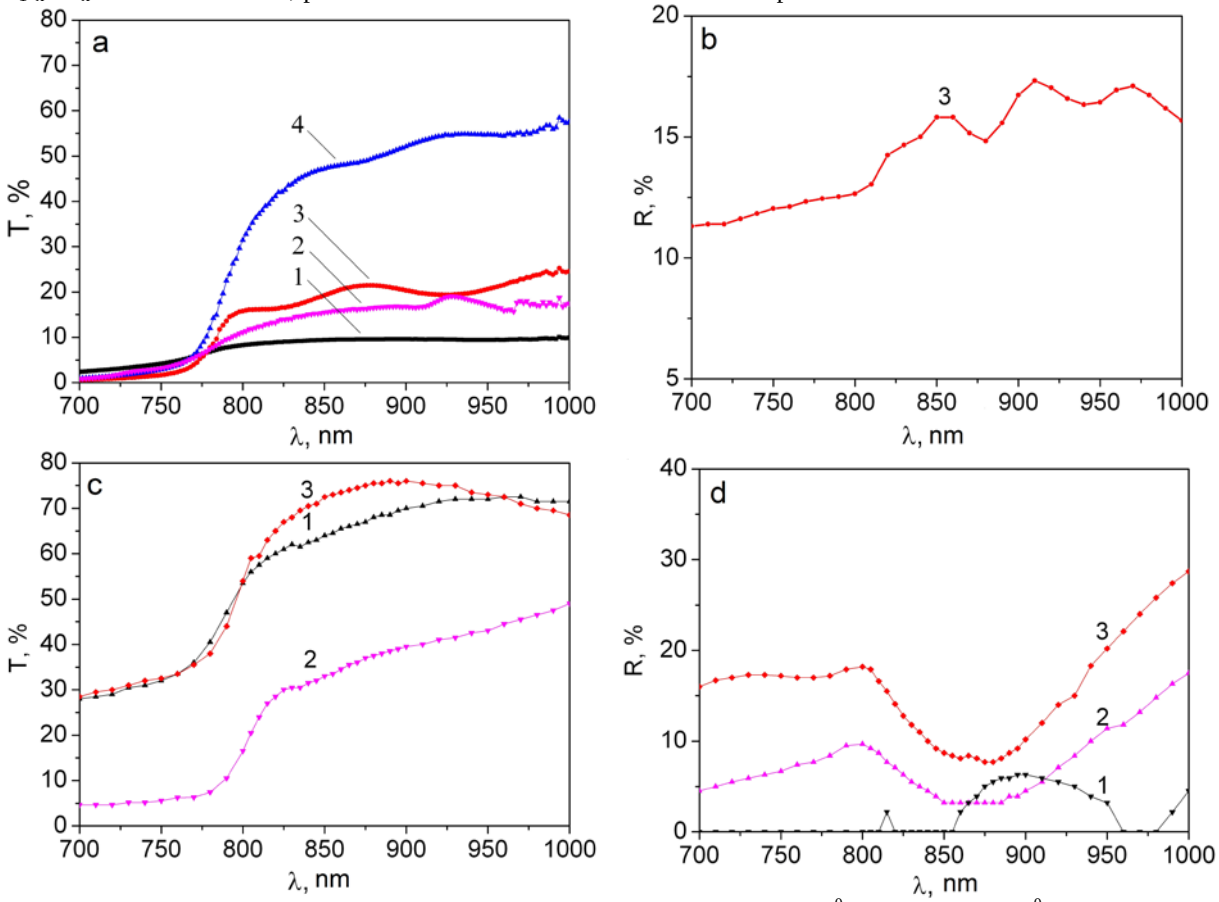

Figure 2. Transmission spectra (a) of the $Cd_{1-x}Mn_xTe$ films, obtained at T_s = 150 ^{0}C and different T_e (^{0}C): 650 (1), 700 (2), 750 (3), 800 (4); reflection spectra (b) T_e = 750 ^{0}C. Transmission- (c) and reflection-spectra (d) of the CdTe thin films – T_e = 620 ^{0}C; T_s, ^{0}C: 200 (1), 300 (2), and 400 (3).

We determined that at a wavelength more than $\lambda \sim$ (720-730) nm, there is a substantial increase in the transmission coefficient (see Fig. 2a); in some cases, the increase was 50-60%. The spectral dependencies of the $R(\lambda)$ and $T(\lambda)$ show an interference minimum and maximum that could be explained by the thinness of the films $l \leq 1.2$ μm.

The absorption coefficient of the $Cd_{1-x}Mn_xTe$films measured for the energy range above the CdTe's BG was α = (1-5)·10^4 cm^{-1}. These values are close to absorption coefficient of the pure CdTe thin films α = (2-5)·10^4 cm^{-1}.

We determined the energy of the BGs of the $Cd_{1-x}Mn_xTe$ and CdTe films from the $(\alpha h\nu)^2 - h\nu$ dependencies (Fig. 3) [25], establishing that it was about 1.5 eV, whereas the E_g of the $Cd_{1-x}Mn_xTe$ films varied from 1.46 to 1.57 eV (see Table 3). Then, we used these experimentally determined E_g values to calculate the concentration of Mn in the $Cd_{1-x}Mn_xTe$ according to concentration dependencies of the BG energy (Eqs. 1 and 2) given in reference [26].

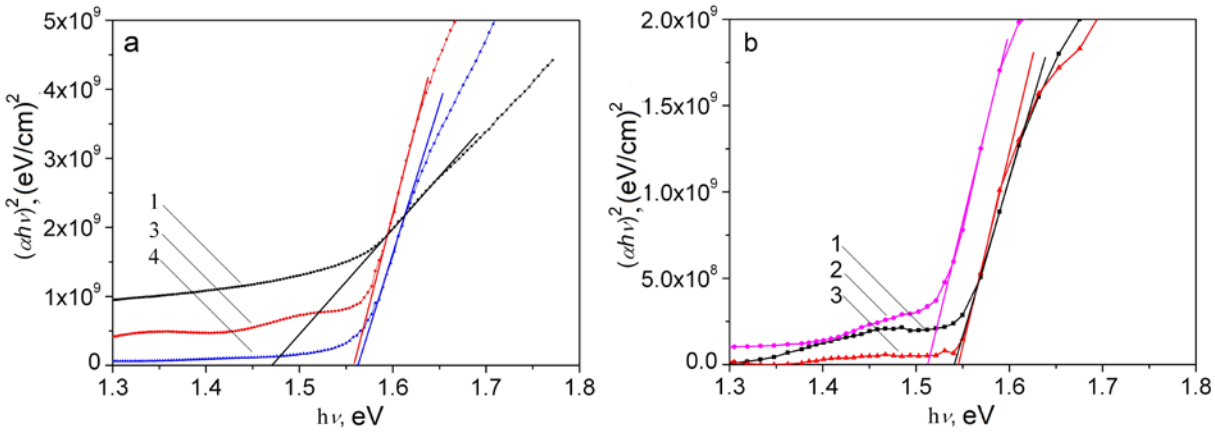

Figure 3. Determination of the BG energy of (a) $Cd_{1-x}Mn_xTe$ and (b) CdTe. The solid solution thin-films obtained from the $Cd_{1-x}Mn_xTe$ powder at T_s=150 ^{0}C and different values of T_e (^{0}C): (a) 650 (1), 750 (3), 800 (4); and (b) CdTe thin films - T_e = 620 ^{0}C; T_s (^{0}C): 200 (1), 300 (2), 400 (3).

Table 3. BG energy and Mn concentration of the $Cd_{1-x}Mn_xTe$ films obtained under different growth conditions; x_1 and x_2 concentrations were calculated according to Eq. 1 and Eq. 2 [26], respectively.

Sample	T_e, ^{0}C	T_s, ^{0}C	E_g, eV	X_1	x_2
1	650	150	1.456	-0.002	0.002
2	700	150	1.480	0.017	0.020
3	750	150	1.561	0.079	0.081
4	800	150	1.565	0.082	0.084

$$E_g = 1{,}458 + 1{,}303x\,, \qquad (1)$$

$$E_g = 1{,}453 + 1{,}34x\,. \qquad (2)$$

As Table 3 shows, the Mn concentration in thin films obtained by the evaporation of the $Cd_{0.7}Mn_{0.3}Te$ powder is very low (x = 0.02-0.08), viz., much lower than the desired Mn concentration (5-6 %) for $Cd_{1-x}Mn_xTe$ bulk detectors. Hence, in order to obtain $Cd_{1-x}Mn_xTe$ films with higher Mn concentration, we co-evaporated CdTe and Mn. Fig. 4 shows the X-ray patterns of the $Cd_{1-x}Mn_xTe$ films deposited by the co-evaporation of the CdTe and Mn. From our structural analysis, we concluded that samples obtained at T_s < 500 ^{0}C correspond to the $Cd_{1-x}Mn_xTe$ solid solution with different Mn concentrations and cubic crystal structures. We note that a reflection from (631) Mn crystal plane was detected on the XRD pattern measured for sample deposited at T_s = 350 ^{0}C; we account for it by the formation of Mn precipitates. Thin films obtained at T_s = 550 ^{0}C have high concentration of hexagonal MnTe precipitates (Fig. 4b), while samples deposited at intermediate substrate temperatures, contain a mixture of $Cd_{1-x}Mn_xTe$- and MnTe-phases.

The Mn concentration in the films obtained by the co-evaporation of the CdTe and Mn was up to 23 at.%, and ratio C_{Cd+Mn}/C_{Te} ranged from 0.94 to 0.98 (Table 2). The average grain size was about 5 μm.

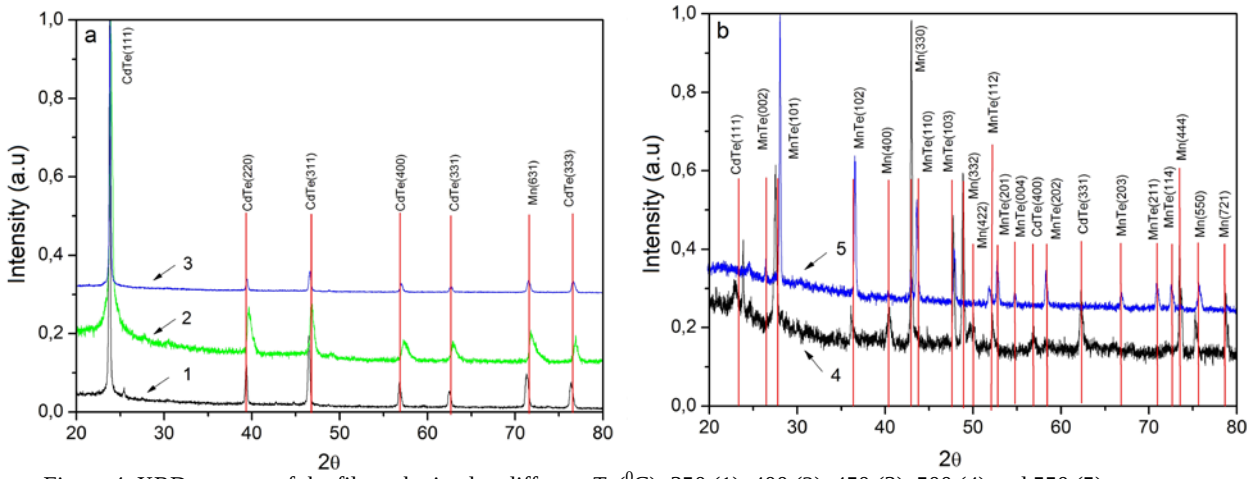

Figure 4. XRD patterns of the films obtained at different T_s (^{0}C): 350 (1), 400 (2), 450 (3), 500 (4) and 550 (5).

CONCLUSIONS

We determined that CdTe films obtained at T_s > (200-250) ^{0}C have a single-phase cubic structure. At lower substrate temperature, we observed traces of the hexagonal phase. The CdTe films have large grain sizes (D = 50-100) μm, coherent scattering-domain sizes L = (56-87) nm, a low rate of micro-deformation (ε = 0.64-1.07), and a low concentration of dislocations ((3.0-7.0)·10^{-14} lin/m^2). From the high crystal quality of these films, we consider them as promising materials for X-ray detectors.

The analysis of the transmission $R(\lambda)$ and reflection spectra $T(\lambda)$ of the films allowed us to determine the band-gap energy (CdTe - E_g = 1.50 eV, $Cd_{1-x}Mn_xTe$ - E_g = (1.46-1.57) eV. The Mn concentration estimated with the help of the reference data for the films obtained from the $Cd_{0.7}Mn_{0.3}Te$ powder was x = 0.02-0.08.

The Mn concentration in the films obtained by the co-evaporation of CdTe and Mn depend on the growth conditions and varied from 0.98 to 25.76 at. %.

ACKNOWLEDGMENTS:

Two of us (Bolotnikov and James) gratefully acknowledge support from the NA-22 Office on Nonproliferation and Treaty Verification.

REFERENCES

[1] Korbutyak, D. V., Melnychuk, S. V., [Cadmium telluride: impurity-defect states and detector properties], Ivan Fedorov, Kyiv, 198 (2000).

[2] Owens, A., Peacock, A., "Compound semiconductor radiation detectors," Nucl. Instrum. Methods 531, 18-37 (2004).

[3] Cui, Y., Bolotnikov, A. E., Hossain, A. et al., "CdMnTe in X-ray and gamma-ray detection: potential applications, Proceedings of SPIE conference on Hard X-ray, Gamma-ray and Neutron Detector Physics X, " SPIE 70790N-1, 2008.

[4] Kim, K. H., Cho, S. H., Suh, J. H., "Gamma-ray response of semi-insulating CdMnTe crystals, "IEEE Nucl. Sci. 56(3), 858-862 (2009).

[5] Ede, A. M. D., Morton, E. J., Antonis P., "Thin-film CdTe for imaging detector applications, "Nucl. Instrum. Methods 458, 7-11 (2001).

[6] Niraula, M., Yasuda, K., Takagi, K., Kusama, H., Tominaga, M., Yamamoto, Y., Agata, Y. and Suzuki, K., "Development of nuclear radiation detectors based on epitaxially grown thick CdTe layers on n+-GaAs substrates, "J. Electr. Materials 34(6), 815-819 (2010).

[7] Kosyachenko, L. A., Rarenko, I. M., Sklyarchuk, V. M., "$Cd_{1-x}Mn_xTe$ as material for radiation and X-ray detectors," Sensor Electronics and Microsystem Technologies 7(1), 74-80 (2010).

[8] Kossut, J., Gaj, J. A., [Introduction to the Physics of Diluted Magnetic Semiconductors], Springer Series in Materials Science, Warsaw, 469 (2010).

[9] Mycielski, A., Kowalczyk, L., Galazka, R.R., "Applications of II–VI semimagnetic semiconductors, "J. Alloy. Comp. 423, 163-168 (2006).

[10] Touat, S. A., Litimein, F., Tadjer, A., "The spin effect of zinc-blende $Cd_{0.5}Mn_{0.5}Te$ and $Zn_{0.5}Mn_{0.5}Te$ diluted magnetic semiconductors: FP-LAPW study, "Physica B 205, 625-631 (2010).

[11] Caricato, A. P., D'Anna, E., Fernandez, M., "Pulsed laser deposition of $Cd_{1-x}Mn_xTe$ thin films", Thin Solid Films 433, 45-49 (2003).

[12] Banerjee, P., Ghosh. B., "Optical and electronic properties of nano-$Cd_{1-x}Mn_xTe$ alloy", J. Phys. Chem. Solids 69, 2670-2673 (2008).

[13] Caraman, I., Rusu, G. I., Leontie, L., "Fundamental absorption edge in thin films of $Cd_{1-x}Mn_xTe$ solid solutions," J. Optoelectron. Advan 8, 927-930 (2006).

[14] Kosyak V. V., Opanasyuk A.S., Bukivskij P. M., Gnatenko Yu. P. "Study of the structural and photoluminescence properties of CdTe polycrystalline films deposited by closed space vacuum sublimation", J. Cryst. Growth 312, 1726–1730 (2010).

[15] Weinberg F, [Devices and methods of physical metallurgy], Mir, Moscow, 427 (1973).

[16] [Selected powder diffraction data for education straining (Search manual and data cards)], International Centre for diffraction data, USA, 432 (1988).

[17] Warren, B. E., [X-ray Diffraction, Dover, New York], 253 (1990).

[18] Bowen, D. K., Brian Tanner, K., [X-Ray Metrology in Semiconductor Manufacturing], Taylor & Francis Group, London, 270 (2006).

[19] Umansky, Ya. S, Skakov, Ju. A., Ivanov, A. N., Rastarguev, L. N. [Crystallography, X-ray and electron microscopy], Metallurgy, Moscow, 632 (1982).

[20] Danilchenko, S. N., Kukharenko, O. G., Moseke, C., Protsenko, I. Yu., Sukhodub, L. F., Sulkio-Cleff, B., "Determination of the Bone Mineral Crystallite Size and Lattice Strain from Diffraction Line Broadening", Cryst. Res. Technol. 37, (2002).

[21] Kurbatov, D., Khlyap, H., Opanasyuk, A., "Substrate-temperature effect on the microstructural and optical properties of ZnS films obtained by close-spaced vacuum sublimation", Phys. Stat. Sol. A 206(7), 1549-1557 (2009).

[22] Kurbatov, D., Kosyak, V., Kolesnyk, M., Opanasyuk, A., Danilchenko, S., "Morphological and structural characteristics of II-VI semiconductor thin films (ZnTe, CdTe, ZnS)", Integrated Ferroelectrics 103(1), 32-40 (2009).

[23] Johansson, S. A. E., Campbell, J. L. and Malmqist, K. G., [Particle-induced X-ray emission spectrometry (PIXE)], John Wiley and Sons, New York, (1995).

[24] Magilin, D. V., Ponomarev, A. G., Rebrov, V. A. "Performance of the Sumy nuclear microprobe with the integrated probe-forming system", Nucl. Instr. and Meth. B 267, 2046-2049 (2009).

[25] Moss, T. S., Balkanski, M., [Handbook on Semiconductors: Optical Properties of Semiconductors], Elsevier, Amsterdam, 857 (1994).
[26] Kim, K. H., Bolotnikov, A. E., Camarda, G. S., Yang, G., Hossain, A., Cui, Y., James, R. B., “Energy-gap dependence on the Mn mole fraction and temperature in CdMnTe crystal”, J. Appl. Phys. 106, 023706-023706-3 (2009).